Single-Cell Signalling Analysis of Heterocellular Organoids

Xiao Qin[1], Jahangir Sufi[1*], Petra Vlckova[1*], Pelagia Kyriakidou[1*], Sophie E. Acton[2], Vivian S. W. Li[3], Mark Nitz[4], and Christopher J. Tape[1,✉]

[1]Cell Communication Lab, Department of Oncology, University College London Cancer Institute, 72 Huntley Street, London, WC1E 6DD, UK.
[2]Stromal Immunology Lab, MRC Laboratory for Molecular Cell Biology, University College London, Gower Street, London, WC1E 6DD, UK.
[3]Stem Cell and Cancer Biology Lab, The Francis Crick Institute, 1 Midland Road, NW1 1AT, UK.
[4]Department of Chemistry, University of Toronto, Toronto, Ontario M5S 3H6, Canada.
[*]These authors contributed equally to this work.

Organoids are biomimetic 3D models of healthy and diseased tissue. Despite their widespread adoption, methods to analyse cell-type specific signalling networks in organoids are absent. Here we report multiplexed single-cell analysis of post-translational modification (PTM) signalling networks in organoids by mass cytometry. Simultaneous analysis of 28 PTMs in >1 million single-organoid cells reveals cell-type and cell-state specific signalling networks in stem, Paneth, enteroendocrine, goblet, tuft cells, and enterocytes during intestinal organoid development. We demonstrate that Thiol-reactive Organoid Barcoding *in situ* (TOB*is*) enables high-throughput multiplexed organoid signalling analysis in a single-tube – opening this technology to single-cell organoid screening. Comparison of colorectal cancer (CRC) oncogenic mutations (*Apc*, *Kras*, and *Trp53*) and tumour microenvironmental cues (fibroblasts and macrophages) revealed CRC driver-mutations mimic signalling normally provided by stromal cells. These results demonstrate mass cytometry is a powerful multiplexed single-cell technology for studying cell-specific signalling in organoid models of healthy and cancerous tissue.

Correspondence: *c.tape@ucl.ac.uk*

Organoids are self-organising 3D tissue models comprising stem and differentiated cells. When compared to traditional 2D cell culture, organoids more accurately represent their parental tissue and are powerful models for study multicellular diseases such as cancer (1). Post-translational modification (PTM) signalling networks underpin fundamental biological phenotypes and are frequently dysregulated in disease (2). To comprehensively explore organoids as models of healthy and diseased tissue, we must be able to quantify PTM signalling networks within organoid cells. Unfortunately, no methods currently exist to study cell-type specific PTM signalling networks in organoids.

We have previously shown that liquid chromatography tandem mass spectrometry (LC-MS/MS) can resolve cell-type specific PTM signalling networks in 2D co-cultures (3). Unfortunately, LC-MS/MS is ill-suited for cell-type specific proteomic analysis of organoids due to abundant contaminating peptides from the protein-rich extracellular matrix (ECM) used in 3D organoid culture. Organoids can be removed from ECM proteins prior to LC-MS/MS analysis – but as physical dissociation of live cells alters cell signalling (4) – PTM measurements from dissociated live organoids do not represent *in situ* cellular states. Moreover, as organoids comprise multiple cell-types (e.g. stem and differentiated) and cell-states (e.g. proliferating, quiescent, and apoptotic), bulk PTM analysis cannot capture the biological heterogeneity present in organoids.

To study signal transduction networks in organoids, we require PTM data that is: 1) cell-type specific, 2) derived from fixed cells, and 3) measures multiple PTMs simultaneously.

Mass cytometry (MC) (also known as cytometry time-of-flight (CyTOF)) uses heavy metal conjugated antibodies to measure >35 proteins in single-cells (5). Although MC is traditionally used for high-dimensional immunophenotyping, MC can also measure PTM signal transduction in heterocellular systems (such as peripheral blood mononuclear cells (PBMCs) (6) and tissues (4)). Given MC's capacity to measure PTMs in mixtures of fixed cells, we theorised that MC could be adapted to study cell-type specific signalling networks in organoids. Here we report the development of a MC workflow to measure single-cell signalling in intestinal organoids (7).

As PTMs can be rapidly altered by cell dissociation (4), we first fix intestinal organoids in Matrigel to preserve cell-signalling. We then physically and enzymatically dissociate fixed organoids into single-cells. We performed a comprehensive screen for intestinal epithelial cell-type identification antibodies (including stem (LGR5, LRIG1, OLFM4), Paneth (Lysozyme), goblet (MUC2, CLCA1), enteroendocrine (CHGA), tuft cells (DCAMKL1), and enterocytes (FABP1, Na/K-ATPase)) that bind fixed antigens and were compatible with rare-earth metal conjugation for MC. Cell-type identification antibodies were further validated by organoid directed differentiation (8) (Supplementary Fig. 1) and integrated into a panel of 28 anti-PTM rare-earth metal antibodies spanning multiple core signalling nodes (Supplementary Table 1) (45 parameters (40 antibodies) / cell). When analysed by MC, this approach enabled us to measure 28 signalling PTMs across 6 cell-types in >1 million single-cells from fixed intestinal organoids (Fig. 1a–c) (Supplementary Fig. 2).

Although organoids are grown in a protein-rich ECM, we found that cell-state probes such as ^{127}5-Iodo-2'-deoxyuridine (^{127}IdU) (identifying S-phase cells (10)) and $^{194/8}$Cisplatin (identifying dead cells (11)) are fully compatible with organoids grown in Matrigel. Combining

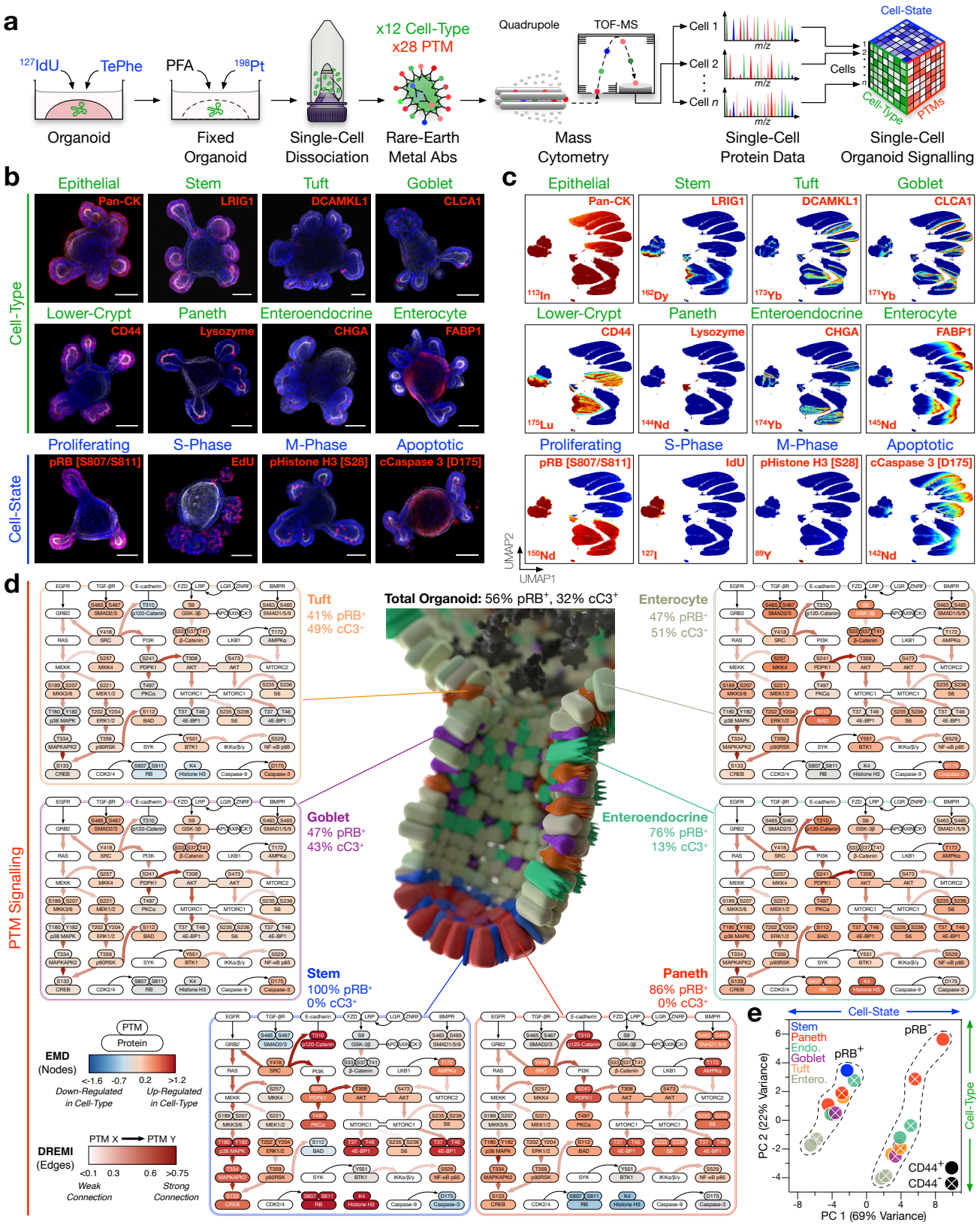

Fig. 1. Single-Cell Signalling Analysis of Intestinal Organoids by Mass Cytometry. a) Experimental workflow. Live organoids are pulsed with ^{127}IdU (S-phase) and TePhe (protein translation), PFA-fixed to preserve signals, stained with ^{198}Cisplatin (dead cells), dissociated into single-cells, stained with 40 rare-earth metal labelled antibodies, and analysed by single-cell MC. **b)** Confocal immunofluorescence (IF) of small intestinal organoids stained with rare-earth metal labelled MC antibodies highlighting individual cell-type and cell-state markers (red), F-Actin (white), and DAPI (blue). Scale bar = 50 µm. (See Supplementary Fig. 1 for directed differentiation antibody validation.) **c)** UMAP (Uniform Manifold Approximation and Projection) (9) distribution of 1 million single-organoid cells analysed by MC. (See Supplementary Fig. 2 for all cell-type, cell-state, and PTM measurements.) **d)** Cell-type specific PTM signalling networks in small intestinal organoids, with nodes coloured by PTM-EMD values describing how different each signalling node is relative to all organoid cells, and arrows coloured by DREMI scores illustrating PTM-PTM connectivity. **e)** PTM-EMD PCA for all organoid cell-types, either proliferating/G0 (pRB$^{+/-}$) or in lower-crypts/villi (CD44$^{+/-}$). Organoid cell signalling is altered by cell-state (PC1) and cell-type (PC2). (See Supplementary Fig. 3 for complete EMD-DREMI signalling maps.)

$^{194/8}$Cisplatin and ^{127}IdU with canonical cell-cycle markers (e.g. pRB [S807/S811], Cyclin B1, and pHistone H3 [S28] (10)) (Supplementary Fig. 2) allowed us to clearly identify live/dead cells and classify single-organoid cells into cell-cycle stages (G0, G1, S-phase, G2, and M-phase (12)) respectively. These cell-state identifiers confirmed that stem and Paneth cells are largely proliferative (pRB$^+$, IdU$^+$/pHH3$^+$, cCaspase3 [D175]$^-$), whereas differentiated epithelia are often post-mitotic (pRB$^-$, IdU$^-$/pHH3$^-$) or apoptotic (cCaspase 3$^+$) (Fig. 1c). Consistent with the finding that intestinal progenitor cells have permissive chromatin *in vivo* (13), proliferating intestinal organoid cells present H3K4me2 (marker of accessible chromatin) whereas post-mitotic cells do not (Supplementary Fig. 2).

To investigate whether stem, Paneth, goblet, enteroendocrine, tuft cells, and enterocytes contain different PTM signalling networks, we combined Earth Mover Distance (EMD) (14) and Density Resampled Estimation of Mutual Information (DREMI) (15) to build cell-type specific signalling networks from single-cell intestinal organoid data (Fig. 1d and Supplementary Fig. 3). In these networks, EMD describes relative PTM intensity (node score) for each organoid cell-type (compared to the total organoid population) and DREMI describes PTM-PTM connectivity (edge score).

EMD-DREMI analysis revealed cell-type specific PTM signalling networks in small intestinal organoids. As canonical WNT signalling is mainly driven by protein interactions, localisation, and degradation (16) (not a classical PTM cascade), MC is not well suited to studying the WNT pathway. Despite this, we observed tertiary evidence of WNT flux (via inhibited pGSK-3β [S9] and non-phosphorylated β-Catenin) in all organoid cell-types (Supplementary Fig. 2). In contrast, MAPK and PI3K pathways displayed cell-type specificity. For example, stem cells channel MAPK signalling through pERK1/2 [T202/Y204], pP90RSK [T359], and pCREB [S133] but fail to connect with pBAD [S112]. In contrast, differentiating epithelia direct MAPK signalling away from pCREB and towards pBAD when proliferating, but lose all MAPK activity in G0 and apoptosis. Stem and Paneth cells also have strong pSRC [Y418] signalling that correlates with downstream PI3K effectors such as pPDPK1 [S241], pPKCα [T497], pAKT [T308] / [S473], and p4E-BP1 [T37/T46]. Notably, Paneth cells have high BMP signalling (via pSMAD1/5 [S463/S465] / SMAD9 [S465/S467]), whereas active TGF-β signalling (via pSMAD2 [S465/S467] / SMAD3 [S423/S425]) is exclusively associated with post-mitotic epithelia (Supplementary Fig. 2).

Several signalling events correlate with cell-state in intestinal organoids. For example, pP38 MAPK [T180/Y182] and pP120-Catenin [T310] are active in all proliferating cells – irrespective of cell-type or location. Similarly, both pAKT [T308] and pMKK4 [S257] (JNK-JUN pathway) are hyperactivated during G2 and M-phase in all cell-types (Supplementary Fig. 2). Principle component analysis (PCA) of PTM-EMDs from proliferating/G0 (pRB$^{+/-}$) and lower-crypts/villi (CD44$^{+/-}$) cells revealed both cell-state (PC1, 69% variance) and, to a lesser extent, cell-type (PC2, 22% variance) describe cell-signalling in small intestinal organoids (Fig. 1e and Supplementary Fig. 3). Collectively, this analysis confirmed MC can identify cell-specific signalling networks in organoids and underscores the importance of single-cell data when studying heterogenous model systems.

In addition to high-dimensional single-cell PTM measurements, a major advantage of MC is the ability to perform multiplexed barcoding of experimental variables (17). Unfortunately, commercially available amine-reactive barcodes (18) bind to abundant ECM proteins used in organoid culture – meaning organoids must be removed from Matrigel before barcoding. Individually removing fixed organoids from Matrigel is a very low-throughput process that limits the scalability of MC multiplexing. We theorised that if organoids could be barcoded *in situ* (i.e. in Matrigel), barcoded organoids could be pooled, dissociated together, and processed as a single high-throughput sample. To explore this idea, we developed a new strategy to barcode organoids while still in Matrigel.

We first used fluorescent probes to investigate how different chemistries bind ECM proteins and organoids in Matrigel. We found that while amine-reactive probes (e.g. NHS Ester) bind lysines and N-terminal amines in ECM proteins, thiol-reactive probes (e.g. C_2 Maleimide) bind exclusively to reduced-cysteines on organoids *in situ* (Supplementary Fig. 4a). We subsequently found that thiol-reactive monoisotopic mass-tagged probes (Maleimide-DOTA-^{157}Gd) also bind organoids *in situ*, whereas amine-reactive probes (NHS Ester-DOTA-^{157}Gd) only react *ex situ* (Supplementary Fig. 4b). This data suggested thiol-reactive chemistries can be used to barcode organoids while still in Matrigel (Supplementary Fig. 4c). Using this knowledge, we developed a 20-plex (*6*-choose-*3*, doublet-filtering (17, 18)) thiol-reactive barcoding strategy based on monoisotopic tellurium maleimide (TeMal) (19) (^{124}Te, ^{126}Te, ^{128}Te, ^{130}Te) and Cisplatin (20) (^{196}Pt, ^{198}Pt) that can bypass Matrigel proteins and bind directly to fixed organoids *in situ* (Supplementary Fig. 4d). This Thiol-reactive Organoid Barcoding *in situ* (TOB*is*) approach enables high-throughput multiplexed single-cell organoid signalling analysis in a single tube (Fig. 2a–b).

As Te and Pt metals are not typically conjugated to antibodies in MC, TOB*is* multiplexing does not compromise the number of antigens measured by MC. Moreover, as barcoding is performed on fixed organoids embedded within Matrigel, TOB*is* does not require the numerous centrifugation or cell membrane permeabilisation steps used in traditional solution-phase barcoding. This greatly increases organoid sample-throughput (Supplementary Fig. 5a–d) and single-cell recovery (Supplementary Fig. 5e–g).

To demonstrate thiol-reactive mass-tagged barcoding can be used to analyse heterogenous organoid cultures, we applied TOB*is* to study cell-type specific epithelial signalling during intestinal organoid development (Fig. 2c) (Supplementary Table 1, 50 parameters (40 antibodies) / cell). Analysis of 28

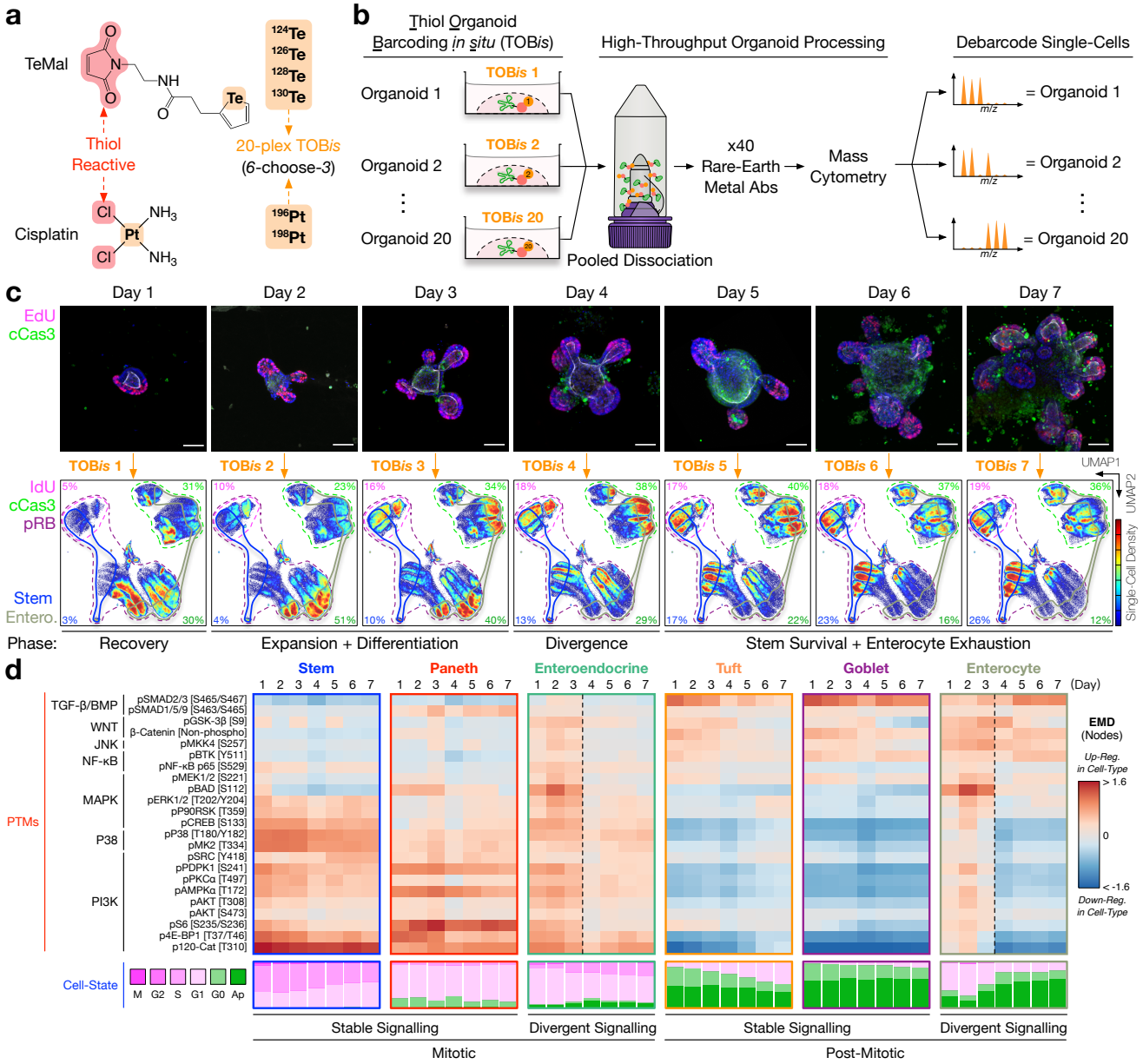

Fig. 2. Thiol-Reactive Organoid Barcoding *in situ* (TOB*is*) for Single-Cell Organoid Multiplexing. a) Thiol-reactive tellurium maleimide (TeMal) (^{124}Te, ^{126}Te, ^{128}Te, ^{130}Te) and Cisplatin (^{196}Pt, ^{198}Pt) isotopologs combined to form a 20-plex (*6-choose-3*) doublet-filtering barcoding strategy. (See Supplementary Fig. 4 for additional details.) **b)** Thiol-reactive Organoid Barcoding *in situ* (TOB*is*) allows organoids to be isotopically barcoded while still in Matrigel and then rapidly processed as a single-sample. (See Supplementary Fig. 5 for additional details.) **c)** Time course of intestinal organoid development illustrating S-phase (EdU$^+$) and apoptotic (cCaspase 3$^+$) cells, scale bar = 50 µm. Each time point was barcoded by TOB*is*, pooled into a single-sample, and analysed by MC. Cell-density UMAP distributions of 2-million single-organoid cells reveal changes in organoid composition across each time point. **d)** Cell-specific PTM-EMDs and cell-state analysis of stem, Paneth, enteroendocrine, tuft, goblet cells, and enterocytes during intestinal organoid development.

PTMs from ~2 million single-organoid cells across 7 days revealed cell-type specific signalling during intestinal organoid development (Fig. 2d).

Multiplexed single-cell analysis demonstrated that after 1 day of culture, organoids seeded as single crypts exist in a 'recovery' phase where ~70% cells have entered the cell-cycle (pRB$^+$), but only <5% have reached S-phase (IdU$^+$) (compared to ~20% in a developed organoid). Days 2 and 3 mark a rapid 'expansion and differentiation' phase of organoid development where stem, Paneth, enteroendocrine cells, and enterocytes activate PI3K, MAPK, and P38 pathways. Despite their strong mitogenic signalling profile, stem cells are unique among proliferating cells in their failure to inhibit BAD. By day 4, intestinal organoids reach a critical 'divergence' phase where crypt and villi signalling digress dramatically. While stem and Paneth cells maintain active PI3K, MAPK, and P38 pathways, enterocytes lose major PI3K (pPDPK1, p4E-BP1, pS6 [S235/S236], pAMPKα [T172], pSRC, pPKCα) and P38 (pP38 MAPK, pMAPKAPK2 [T334], pCREB) node activity. As a result, by days 5–7 the majority of enterocytes are either post-mitotic (pRB$^-$) or apoptotic (cCaspase3$^+$), with increased TGF-β signalling, while stem cells retain cell-cycle activity. Consequently, stem cell number increases and enterocytes become exhausted at

the end of intestinal organoid development. Stem and Paneth cells continue to display high PI3K, MAPK, and P38 activity even at this late phase of culture. This suggests maintaining a stable signalling flux is a core feature of intestinal crypt cells. In contrast, tuft and goblet cells display high TGF-β signalling, low PI3K-MAPK-P38 activity, and low cell-cycle activity throughout organoid development. This implies that irrespective of organoid age, tuft and goblet cells shut down major mitotic signalling pathways once differentiated. Collectively, this data reveals cell-type specific signalling during intestinal organoid development and confirms TOB*is* can be used to perform multiplexed single-cell signalling analysis of heterogenous organoid cultures.

We have demonstrated how a modified MC workflow can enable high-throughput multiplexed single-cell analysis of signalling networks in epithelial organoids. However, as MC can theoretically resolve any cell-type, we hypothesised that this technology could be expanded to study cell-signalling in more complex organoid tissue models comprising epithelial, stromal, and immune cells. To test this, we developed a heterocellular organoid model of the colorectal cancer (CRC) tumour microenvironment (21) comprising colonic epithelial organoids (Supplementary Fig. 6a), colonic fibroblasts (Supplementary Fig. 6b), and bone marrow-derived macrophages (Supplementary Fig. 6c). Stromal fibroblasts have emerged as a major driver of CRC (22, 23) and macrophages, the most abundant leukocyte in the colon (24), can promote CRC metastasis (25).

CRC develops through successive oncogenic mutations – often resulting in loss of APC activity, activation of KRAS, and perturbation of TP53 (26). While the underlying driver mutations of CRC have been well studied, how they deregulate epithelial signalling relative to cues from stromal and immune cells is unclear. To investigate this, we cultured wild-type (WT), *shApc* (A), *shApc* and *Kras*$^{G12D/+}$ (AK), or *shApc*, *Kras*$^{G12D/+}$, and *Trp53*$^{R172H/-}$ (AKP) (27, 28) colonic epithelial organoids either alone, with colonic fibroblasts, and/or macrophages. Each CRC genotype-microenvironment organoid culture was fixed, TOB*is*-barcoded, and single-cell signalling analysis was performed in one multiplexed MC run (Fig. 3a–b) (Supplementary Table 2, 50 parameters (40 antibodies) / cell).

Addition of myeloid (CD68 and F4/80) and mesenchymal (Podoplanin) heavy metal antibodies enabled clear resolution of epithelial organoids, macrophages, and fibroblasts from each condition (Fig. 3c). EMD-PTM PCA of organoids (Fig. 3d), macrophages (Fig. 3e), and fibroblasts (Fig. 3f) revealed cell-type specific signalling profiles across all genotype and microenvironment conditions.

As expected, oncogenic mutations have a large effect on organoid signalling. However, we also observed microenvironmental cues have a comparable impact on organoid signalling to oncogenic mutations (discussed in detail below). Although oncogenic mutations cell-autonomously upregulate many signalling nodes, stromal cells can further upregulate mutated CRC organoid signalling via PI3K (pS6, p4E-BP1, and pAKT) and JNK (pMKK4) pathways (Supplementary Fig. 7). Microenvironmental activation of these nodes may contribute towards the poor-prognosis of CRC patients with highly stromal tumours (22, 23).

We also observed unreported polarity in cell-cell communication. For example, macrophage signalling pathways (MAPK, PI3K, and NF-κB) are heavily upregulated by fibroblasts (Fig. 3e), whereas fibroblast signalling is scarcely altered by macrophages (Fig. 3f). In contrast, fibroblast MAPK and P38 signalling is mainly upregulated by epithelial cells, which in turn, reciprocally benefit from fibroblasts (Supplementary Fig. 8). These results suggest colonic fibroblasts are major regulators of intercellular signalling in the colonic microenvironment.

To further investigate the relationship between genotypic and microenvironmental regulation of epithelial signalling, we overlaid single-cell MC data from WT, A, AK, and AKP organoids onto a microenvironmental Scaffold map (29) constructed from WT colonic organoids alone or co-cultured with colonic fibroblasts and/or macrophages (Fig. 3g) (Supplementary Fig. 9). This Scaffold analysis confirmed A, AK, and AKP mutations mimic the signalling profile of WT organoids in the presence of stromal cells. (Inverted organoid genotype Scaffold maps also revealed a striking similarity between mutation- and microenvironment-driven signalling (Supplementary Fig. 10)). Direct comparison of organoid PTM signalling revealed both PI3K/PKC (pPDPK1, pPKCα, pAKT, p4E-BP1, pS6, pSRC, pP120-Catenin, and pAMPKα) and P38/MAPK (pP38 MAPK, pMAPKAPK2, pP90RSK, pCREB, and pBAD) nodes are analogously upregulated by oncogenic mutations and microenvironmental cues (Fig. 3h). In contrast, epithelial signalling network connectivity is regulated by genotype, not microenvironment (Supplementary Fig. 11).

These results indicate that in CRC: 1) oncogenic mutations mimic an epithelial signalling state normally driven by stromal cells, and 2) oncogenic mutations fundamentally restructure signalling networks in cancer cells, whereas microenvironmental cues drive acute signalling flux. Collectively, this analysis confirms MC can be used to study cell-type specific signalling across epithelial, stromal, and immune cells in heterocellular 3D organoid models of the tumour microenvironment.

We have described a workflow to perform multiplexed single-cell signalling analysis of heterocellular organoids using MC. While this study has focused on intestinal organoids, we expect this technology to be fully compatible with organoids derived from other tissues (e.g. brain, liver, pancreas, kidney etc). Cell-type identification antibodies for each tissue should be carefully validated, but otherwise the TOB*is* multiplexing and PTM analysis framework we report should be compatible with all organoids (including those grown in defined-hydrogels).

In addition to general single-cell organoid signalling experiments, the technology reported here holds substantial promise for organoid screening. It has recently been shown that high-throughput drug screening of patient-derived organoids (PDOs) can inform clinical treatment of cancer

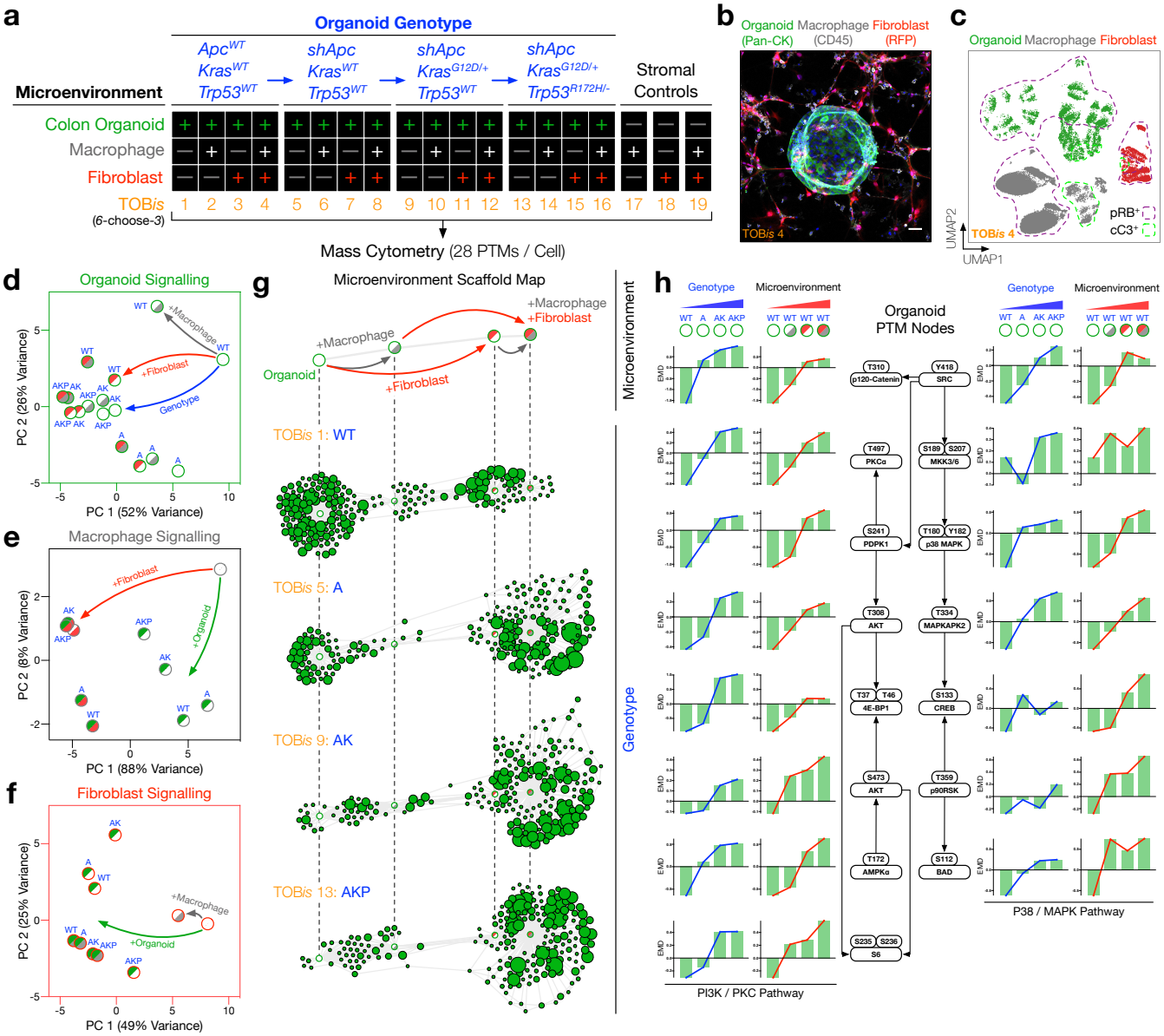

Fig. 3. Single-Cell Signalling Analysis of CRC Tumour Microenvironment Organoids. a) CRC organoid genotypes (wild-type (WT), *shApc* (A), *shApc* and *Kras*$^{G12D/+}$ (AK), *shApc*, *Kras*$^{G12D/+}$, and *Trp53*$^{R172H/-}$ (AKP)) cultured in the presence or absence of colonic fibroblasts and/or macrophages. Each condition was barcoded using TOB*is* and analysed by single-cell MC (40 antibodies / cell). **b)** Confocal IF of a WT colonic organoid (Pan-CK, green) co-cultured with colonic fibroblasts (RFP, red), and macrophages (CD45, grey) (TOB*is* 4), scale bar = 50 µm. **c)** UMAP distribution of the colonic microenvironment model identifies single epithelial cells, fibroblasts, and macrophages (TOB*is* 4). **d)** PTM-EMD PCA for colonic epithelial organoids, **e)** macrophages, and **f)** fibroblasts across all genotype / microenvironment combinations. **g)** Scaffold maps constructed from WT organoids either alone or in co-culture with colonic fibroblasts and/or macrophages. Unsupervised distribution of A, AK, and AKP colonic organoids revealed oncogenic mutations mimic the signalling profile driven by stromal microenvironments. (See Supplementary Fig. 9 for all genotype / microenvironment combinations and Supplementary Fig. 10 for mutation-driven Scaffold maps.) **h)** PTM-EMDs for organoid PI3K/PKC and P38/MAPK signalling nodes following genotypic and microenvironmental regulation. (See Supplementary Fig. 11 for DREMI edge scores.)

(30, 31). While monoculture organoid screens have shown exceptional promise, their reliance on bulk viability measurements (e.g. CellTiter-Blue) means they cannot evaluate drugs targeting stromal and/or immune cells (including immunotherapies) and cannot provide any mechanistic understanding of drug performance and/or resistance. In contrast, a TOB*is* multiplexed MC drug screen would describe cell-type specific signalling networks, cell-cycle states, and apoptotic readouts at single-cell resolution across all cells in PDO co-cultures (including air-liquid interface tumour microenvironment organoids (32)). Future development of TOB*is* barcodes (using additional TeMal/Cisplatin isotopologs and maleimide-DOTA-metal conjugates) will greatly expand organoid multiplexing capacity and advance this technology to high-throughput organoid screening applications.

METHODS

Methods, including statements of data availability and any associated accession codes and references, are available in the online version of the paper.

ACKNOWLEDGEMENTS

We are extremely grateful to Dr. Lukas Dow (Cornell University) for sharing CRC organoids, Dr. Xin Lu (University of Oxford) for sharing mouse intestines, and Dr. Olga Ornatsky (Fluidigm) for proving monoisotopic Cisplatin (^{195}Pt and ^{196}Pt). We thank the UCL CI Flow-Core for MC support and Dr. Leland McInnes (Tutte Institute) for UMAP advise. Graphical organoid renders were designed by Dr. Jeroen Claus (Phospho Biomedical Animation). This work was supported by Cancer Research UK (C60693/A23783), UCLH Biomedical Research Centre (BRC422), The Royal Society (RSG\Rd1\180234), and Rosetrees Trust (A1989).

AUTHOR CONTRIBUTIONS

X.Q. Designed the study, performed organoid and MC experiments, analysed the data, and wrote the paper.
J.S. Developed TOB*is*, designed rare-earth metal antibody panels, performed MC analysis, and analysed data.
P.V. Isolated and characterised colonic fibroblasts, macrophages, cultured organoids, and analysed data.
P.K. Performed UMAP, EMD, DREMI, and PCA data analysis.
M.N. Developed TeMal barcodes.
S.A. Provided murine monocytes and intestines for fibroblast isolation.
V.L. Provided murine small intestines for organoid isolation.
C.T. Designed the study, analysed the data, and wrote the paper.

COMPETING INTERESTS

M.N. has pending intellectual property on the use of tellurium reagents for mass cytometry applications which has been licensed to Fluidigm Corporation.

REFERENCES

1. H. Clevers. Modeling development and disease with organoids. *Cell*, 165(7):1586–1597, 2016.
2. T. Pawson and J. D. Scott. Protein phosphorylation in signaling–50 years and counting. *Trends Biochem Sci*, 30(6):286–90, 2005.
3. C. J. Tape, S. Ling, M. Dimitriadi, K. M. McMahon, J. D. Worboys, H. S. Leong, I. C. Norrie, C. J. Miller, G. Poulogiannis, D. A. Lauffenburger, and C. Jorgensen. Oncogenic kras regulates tumor cell signaling via stromal reciprocation. *Cell*, 165(4):910–20, 2016.
4. A. J. Simmons, A. Banerjee, E. T. McKinley, C. R. Scurrah, C. A. Herring, L. S. Gewin, R. Masuzaki, S. J. Karp, J. L. Franklin, M. J. Gerdes, J. M. Irish, R. J. Coffey, and K. S. Lau. Cytometry-based single-cell analysis of intact epithelial signaling reveals mapk activation divergent from tnf-alpha-induced apoptosis in vivo. *Mol Syst Biol*, 11(10):835, 2015.
5. M. H. Spitzer and G. P. Nolan. Mass cytometry: Single cells, many features. *Cell*, 165(4): 780–91, 2016.
6. S. C. Bendall, E. F. Simonds, P. Qiu, A. D. Amir el, P. O. Krutzik, R. Finck, R. V. Bruggner, R. Melamed, A. Trejo, O. I. Ornatsky, R. S. Balderas, S. K. Plevritis, K. Sachs, D. Pe'er, S. D. Tanner, and G. P. Nolan. Single-cell mass cytometry of differential immune and drug responses across a human hematopoietic continuum. *Science*, 332(6030):687–96, 2011.
7. T. Sato, R. G. Vries, H. J. Snippert, M. van de Wetering, N. Barker, D. E. Stange, J. H. van Es, A. Abo, P. Kujala, P. J. Peters, and H. Clevers. Single lgr5 stem cells build crypt-villus structures in vitro without a mesenchymal niche. *Nature*, 459(7244):262–5, 2009.
8. X. Yin, H. F. Farin, J. H. van Es, H. Clevers, R. Langer, and J. M. Karp. Niche-independent high-purity cultures of lgr5+ intestinal stem cells and their progeny. *Nat Methods*, 11(1): 106–12, 2014.
9. L. McInnes and J. Healy. Umap: Uniform manifold approximation and projection for dimension reduction. *arXiv*, 2018.
10. G. K. Behbehani, S. C. Bendall, M. R. Clutter, W. J. Fantl, and G. P. Nolan. Single-cell mass cytometry adapted to measurements of the cell cycle. *Cytometry A*, 81(7):552–66, 2012.
11. H. G. Fienberg, E. F. Simonds, W. J. Fantl, G. P. Nolan, and B. Bodenmiller. A platinum-based covalent viability reagent for single-cell mass cytometry. *Cytometry A*, 81(6):467–75, 2012.
12. M. A. Rapsomaniki, X. K. Lun, S. Woerner, M. Laumanns, B. Bodenmiller, and M. R. Martinez. Cellcycletracer accounts for cell cycle and volume in mass cytometry data. *Nat Commun*, 9(1):632, 2018.
13. T. H. Kim, F. Li, I. Ferreiro-Neira, L. L. Ho, A. Luyten, K. Nalapareddy, H. Long, M. Verzi, and R. A. Shivdasani. Broadly permissive intestinal chromatin underlies lateral inhibition and cell plasticity. *Nature*, 506(7489):511–5, 2014.
14. J. H. Levine, E. F. Simonds, S. C. Bendall, K. L. Davis, A. D. Amir el, M. D. Tadmor, O. Litvin, H. G. Fienberg, A. Jager, E. R. Zunder, R. Finck, A. L. Gedman, I. Radtke, J. R. Downing, D. Pe'er, and G. P. Nolan. Data-driven phenotypic dissection of aml reveals progenitor-like cells that correlate with prognosis. *Cell*, 162(1):184–97, 2015.
15. S. Krishnaswamy, M. H. Spitzer, M. Mingueneau, S. C. Bendall, O. Litvin, E. Stone, D. Pe'er, and G. P. Nolan. Systems biology. conditional density-based analysis of t cell signaling in single-cell data. *Science*, 346(6213):1250689, 2014.
16. R. Nusse and H. Clevers. Wnt/beta-catenin signaling, disease, and emerging therapeutic modalities. *Cell*, 169(6):985–999, 2017.
17. B. Bodenmiller, E. R. Zunder, R. Finck, T. J. Chen, E. S. Savig, R. V. Bruggner, E. F. Simonds, S. C. Bendall, K. Sachs, P. O. Krutzik, and G. P. Nolan. Multiplexed mass cytometry profiling of cellular states perturbed by small-molecule regulators. *Nat Biotechnol*, 30(9): 858–67, 2012.
18. E. R. Zunder, R. Finck, G. K. Behbehani, A. D. Amir el, S. Krishnaswamy, V. D. Gonzalez, C. G. Lorang, Z. Bjornson, M. H. Spitzer, B. Bodenmiller, W. J. Fantl, D. Pe'er, and G. P. Nolan. Palladium-based mass tag cell barcoding with a doublet-filtering scheme and single-cell deconvolution algorithm. *Nat Protoc*, 10(2):316–33, 2015.
19. L. M. Willis, H. Park, M. W. L. Watson, D. Majonis, J. L. Watson, and M. Nitz. Tellurium-based mass cytometry barcode for live and fixed cells. *Cytometry A*, 2018.
20. R. L. McCarthy, D. H. Mak, J. K. Burks, and M. C. Barton. Rapid monoisotopic cisplatin based barcoding for multiplexed mass cytometry. *Sci Rep*, 7(1):3779, 2017.
21. C. J. Tape. The heterocellular emergence of colorectal cancer. *Trends Cancer*, 3(2):79–88, 2017.
22. A. Calon, E. Lonardo, A. Berenguer-Llergo, E. Espinet, X. Hernando-Momblona, M. Iglesias, M. Sevillano, S. Palomo-Ponce, D. V. Tauriello, D. Byrom, C. Cortina, C. Morral, C. Barcelo, S. Tosi, A. Riera, C. S. Attolini, D. Rossell, E. Sancho, and E. Batlle. Stromal gene expression defines poor-prognosis subtypes in colorectal cancer. *Nat Genet*, 47(4):320–9, 2015.
23. C. Isella, A. Terrasi, S. E. Bellomo, C. Petti, G. Galatola, A. Muratore, A. Mellano, R. Senetta, A. Cassenti, C. Sonetto, G. Inghirami, L. Trusolino, Z. Fekete, M. De Ridder, P. Cassoni, G. Storme, A. Bertotti, and E. Medico. Stromal contribution to the colorectal cancer transcriptome. *Nat Genet*, 47(4):312–9, 2015.
24. A. M. Mowat and W. W. Agace. Regional specialization within the intestinal immune system. *Nat Rev Immunol*, 14(10):667–85, 2014.
25. J. Lan, L. Sun, F. Xu, L. Liu, F. Hu, D. Song, Z. Hou, W. Wu, X. Luo, J. Wang, X. Yuan, J. Hu, and G. Wang. M2 macrophage-derived exosomes promote cell migration and invasion in colon cancer. *Cancer Res*, 2018.
26. Network Cancer Genome Atlas. Comprehensive molecular characterization of human colon and rectal cancer. *Nature*, 487(7407):330–7, 2012.
27. L. E. Dow, K. P. O'Rourke, J. Simon, D. F. Tschaharganeh, J. H. van Es, H. Clevers, and S. W. Lowe. Apc restoration promotes cellular differentiation and reestablishes crypt homeostasis in colorectal cancer. *Cell*, 161(7):1539–1552, 2015.
28. K. P. O'Rourke, E. Loizou, G. Livshits, E. M. Schatoff, T. Baslan, E. Manchado, J. Simon, P. B. Romesser, B. Leach, T. Han, C. Pauli, H. Beltran, M. A. Rubin, L. E. Dow, and S. W. Lowe. Transplantation of engineered organoids enables rapid generation of metastatic mouse models of colorectal cancer. *Nat Biotechnol*, 35(6):577–582, 2017.
29. M. H. Spitzer, P. F. Gherardini, G. K. Fragiadakis, N. Bhattacharya, R. T. Yuan, A. N. Hotson, R. Finck, Y. Carmi, E. R. Zunder, W. J. Fantl, S. C. Bendall, E. G. Engleman, and G. P. Nolan. Immunology. an interactive reference framework for modeling a dynamic immune system. *Science*, 349(6244):1259425, 2015.
30. M. van de Wetering, H. E. Francies, J. M. Francis, G. Bounova, F. Iorio, A. Pronk, W. van Houdt, J. van Gorp, A. Taylor-Weiner, L. Kester, A. McLaren-Douglas, J. Blokker, S. Jaksani, S. Bartfeld, R. Volckman, P. van Sluis, V. S. Li, S. Seepo, C. Sekhar Pedamallu, K. Cibulskis, S. L. Carter, A. McKenna, M. S. Lawrence, L. Lichtenstein, C. Stewart, J. Koster, R. Versteeg, A. van Oudenaarden, J. Saez-Rodriguez, R. G. Vries, G. Getz, L. Wessels, M. R. Stratton, U. McDermott, M. Meyerson, M. J. Garnett, and H. Clevers. Prospective derivation of a living organoid biobank of colorectal cancer patients. *Cell*, 161(4):933–45, 2015.
31. G. Vlachogiannis, S. Hedayat, A. Vatsiou, Y. Jamin, J. Fernandez-Mateos, K. Khan, A. Lampis, K. Eason, I. Huntingford, R. Burke, M. Rata, D. M. Koh, N. Tunariu, D. Collins, S. Hulkki-Wilson, C. Ragulan, I. Spiteri, S. Y. Moorcraft, I. Chau, S. Rao, D. Watkins, N. Fotiadis, M. Bali, M. Darvish-Damavandi, H. Lote, Z. Eltahir, E. C. Smyth, R. Begum, P. A. Clarke, J. C. Hahne, M. Dowsett, J. de Bono, P. Workman, A. Sadanandam, M. Fassan, O. J. Sansom, S. Eccles, N. Starling, C. Braconi, A. Sottoriva, S. P. Robinson, D. Cunningham, and N. Valeri. Patient-derived organoids model treatment response of metastatic gastrointestinal cancers. *Science*, 359(6378):920–926, 2018.
32. J. T. Neal, X. Li, J. Zhu, V. Giangarra, C. L. Grzeskowiak, J. Ju, I. H. Liu, S. H. Chiou, A. A. Salahudeen, A. R. Smith, B. C. Deutsch, L. Liao, A. J. Zemek, F. Zhao, K. Karlsson, L. M. Schultz, T. J. Metzner, L. D. Nadauld, Y. Y. Tseng, S. Alkhairy, C. Oh, P. Keskula, D. Mendoza-Villanueva, F. M. De La Vega, P. L. Kunz, J. C. Liao, J. T. Leppert, J. B. Sunwoo, C. Sabatti, J. S. Boehm, W. C. Hahn, G. X. Y. Zheng, M. M. Davis, and C. J. Kuo. Organoid modeling of the tumor immune microenvironment. *Cell*, 175(7):1972–1988 e16, 2018.